

The Role of Flow-Independent Viscoelasticity in the Biphasic Tensile and Compressive Responses of Articular Cartilage

Chun-Yuh Huang
Van C. Mow
Gerard A. Ateshian

Departments of Mechanical Engineering and
Biomedical Engineering,
Columbia University,
New York, NY 10027

A long-standing challenge in the biomechanics of connective tissues (e.g., articular cartilage, ligament, tendon) has been the reported disparities between their tensile and compressive properties. In general, the intrinsic tensile properties of the solid matrices of these tissues are dictated by the collagen content and microstructural architecture, and the intrinsic compressive properties are dictated by their proteoglycan content and molecular organization as well as water content. These distinct materials give rise to a pronounced and experimentally well-documented nonlinear tension–compression stress–strain responses, as well as biphasic or intrinsic extracellular matrix viscoelastic responses. While many constitutive models of articular cartilage have captured one or more of these experimental responses, no single constitutive law has successfully described the uniaxial tensile and compressive responses of cartilage within the same framework. The objective of this study was to combine two previously proposed extensions of the biphasic theory of Mow et al. [1980, ASME J. Biomech. Eng., 102, pp. 73–84] to incorporate tension–compression nonlinearity as well as intrinsic viscoelasticity of the solid matrix of cartilage. The biphasic-conewise linear elastic model proposed by Soltz and Ateshian [2000, ASME J. Biomech. Eng., 122, pp. 576–586] and based on the bimodular stress–strain constitutive law introduced by Curnier et al. [1995, J. Elasticity, 37, pp. 1–38], as well as the biphasic poroviscoelastic model of Mak [1986, ASME J. Biomech. Eng., 108, pp. 123–130], which employs the quasi-linear viscoelastic model of Fung [1981, Biomechanics: Mechanical Properties of Living Tissues, Springer-Verlag, New York], were combined in a single model to analyze the response of cartilage to standard testing configurations. Results were compared to experimental data from the literature and it was found that a simultaneous prediction of compression and tension experiments of articular cartilage, under stress-relaxation and dynamic loading, can be achieved when properly taking into account both flow-dependent and flow-independent viscoelasticity effects, as well as tension–compression nonlinearity. [DOI: 10.1115/1.1392316]

Introduction

Over the past two decades, several studies have established that the viscous drag induced by interstitial fluid flowing within the porous-permeable collagen–proteoglycan matrix of cartilage imparts viscoelasticity to the mechanical response of this tissue. This flow-dependent viscoelastic phenomenon has been the basis of successful porous media models [1–7], which can describe the response of articular cartilage under various compressive loading conditions, including confined [1,2,4] and unconfined [7,8] compression of cylindrical cartilage discs, as well as indentation of cartilage layers with a flat or spherical indenter [9,10]. In addition to this mechanism of flow-dependent viscoelasticity, some investigators have proposed that there also exists an intrinsic, flow-independent viscoelasticity in the solid matrix [11,12], leading to the formulation and application of porous media models with a viscoelastic solid phase [13–15]. Incorporation of intrinsic viscoelasticity into porous media models has often produced better agreement between theory and experiments than in the absence of modeling such effects [16,17], though not always [18].

However, it has been difficult to assess whether this improved agreement has indeed resulted from the existence of intrinsic solid–matrix viscoelasticity, or was caused by the increased math-

ematical flexibility of the governing equations and the number of material parameters in the model. A long-standing argument in favor of the former interpretation has been the experimental observation of a frequency-dependent response in the dynamic shear loading of cartilage [11,12,19,20]; indeed, porous media models of isotropic materials undergoing infinitesimal deformation predict an isochoric deformation under torsional shear, which would preclude interstitial fluid pressurization and flow. Thus, the observation of a viscoelastic response in torsional shear should support the premise of intrinsic viscoelasticity of the solid matrix [11,19]. However, it is important to recognize the limiting assumptions of this analysis, namely that cartilage is not necessarily isotropic and that for certain classes of anisotropy torsional shear can produce nonzero dilatation, and that the prediction of isochoric deformation under infinitesimal strain is a mathematical idealization that neglects higher order deformation effects that remain present experimentally (i.e., higher order changes in dilatation may produce non-negligible interstitial fluid pressurization and flow).

Another confounding factor in the assessment of intrinsic solid matrix viscoelasticity has been the observation that other modeling assumptions of cartilage can equally improve agreement between theoretical predictions and experimental data. For example, in confined and unconfined compression and indentation, good agreement with experiments has been found not only with linear isotropic poroviscoelastic biphasic models [14,17,21], but also when using a linear transversely isotropic biphasic model [8,9,10], or nonlinear bimodular biphasic models [7,22]. Modeling the in-

Contributed by the Bioengineering Division for publication in the JOURNAL OF BIOMECHANICAL ENGINEERING. Manuscript received by the Bioengineering Division December 13, 2000; revised manuscript received May 16, 2001. Associate Editor: L. A. Setton.

homogeneity of cartilage observed in compression [23–25] similarly appears to have a potential for improving agreement between the isotropic biphasic theory and experimental data in confined and unconfined compression [26,27].

In our own studies, we have been able to demonstrate good agreement between the infinitesimal or finite deformation isotropic biphasic models [1,28] and experiments in confined compression creep and stress-relaxation [4,29], and dynamic loading [18], not only by curve-fitting the corresponding experimental load or deformation response but also by predicting the measured interstitial fluid pressurization. For unconfined compression of cylindrical samples of cartilage, where the tissue is simultaneously subjected to axial compression and radial and circumferential tension [30], we have recently proposed to incorporate the Conewise Linear Elasticity (CLE) model of Curnier et al. [31] into the biphasic theory of Mow et al. [1] to account for the disparity in the tensile and compressive moduli of articular cartilage observed in various studies (e.g., [1,4,32–39]). This model was shown to produce good agreement between theory and experiments in unconfined compression, including in its ability to predict the cartilage interstitial fluid response [22]. However, an interesting prediction of this biphasic-CLE model, which is presented below, is that the response of cartilage under uniaxial tension (an experimental configuration often investigated in the literature [32,33,35–38,40] but not yet predicted successfully with a porous media model) exhibits almost no transient response, unlike experimental observations [35,37,40]. This finding suggests that uniaxial tension of articular cartilage may indeed be a discriminating testing configuration for investigating the intrinsic viscoelasticity of the solid matrix of articular cartilage, in the context of a porous media model that also describes the tension-compression nonlinearity of articular cartilage.

Therefore, the short-term objective of this study is to understand the role of flow-independent viscoelasticity in the context of a porous media model of cartilage which accounts for its tension-compression nonlinearity. The long-term objective is to develop a more comprehensive framework for understanding the mechanical behavior of cartilage than the currently available theoretical models, which can better interpret the diverse experimental outcomes reported in the literature; this framework should further help explain how cartilage is able to sustain the high compressive stresses typical of *in vivo* loading conditions that far exceed its equilibrium compressive modulus [41,42]. The specific aims are to combine existing theories of cartilage that incorporate intrinsic viscoelasticity and tension-compression nonlinearity of the solid matrix within a biphasic model; and to investigate the response of such a model to standard testing configurations and compare the outcomes to experimental data reported in the literature.

Model Formulation

Mak [13] developed a formulation for an isotropic biphasic model of cartilage whose solid phase is described by the quasi-linear viscoelasticity (QLV) theory of Fung [43], with the tissue modeled as a binary mixture of an intrinsically incompressible solid phase, representing primarily the collagen fibers, proteoglycans, and chondrocytes, and an intrinsically incompressible fluid phase representing the interstitial water [1]. The governing equations for this model, known as the biphasic poroviscoelastic (BPVE) theory, are the momentum equation for the mixture (neglecting inertia and in the absence of body forces),

$$\nabla \cdot \boldsymbol{\sigma} = -\nabla p + \nabla \cdot \boldsymbol{\sigma}^{ve} = \mathbf{0}, \quad (1)$$

where $\boldsymbol{\sigma}$ represents the total stress tensor, which is the sum of the interstitial fluid pressure p and the viscoelastic or effective stress $\boldsymbol{\sigma}^{ve}$ resulting from deformation of the solid matrix ($\boldsymbol{\sigma} = -p\mathbf{I} + \boldsymbol{\sigma}^{ve}$), $\nabla \cdot$ denotes the divergence operator, and ∇ is the gradient operator; and the continuity equation for the mixture,

$$\nabla \cdot (\mathbf{v}^s + \mathbf{w}) = 0, \quad (2)$$

where $\mathbf{w} = \varphi^f(\mathbf{v}^f - \mathbf{v}^s)$ is the flux of fluid relative to the solid, φ^f is the fluid volume fraction (tissue porosity) and $\mathbf{v}^s, \mathbf{v}^f$ are the solid and fluid phase velocities, respectively. In one of the simpler embodiments of the QLV theory,¹ the viscoelastic stress tensor $\boldsymbol{\sigma}^{ve}$ can be related to the stress tensor under equilibrium conditions, $\boldsymbol{\sigma}^e$, through

$$\boldsymbol{\sigma}^{ve}(t) = g(t)\boldsymbol{\sigma}^e[\mathbf{E}(0)] + \int_0^t g(t-\tau) \frac{\partial \boldsymbol{\sigma}^e}{\partial \tau}[\mathbf{E}(\tau)] d\tau. \quad (3)$$

The infinitesimal strain tensor \mathbf{E} , which appears above, is related to the solid displacement \mathbf{u} through $\mathbf{E} = (1/2)(\nabla \mathbf{u} + \nabla \mathbf{u}^T)$, and the displacement to the solid velocity through $\mathbf{v}^s = D^s \mathbf{u} / Dt$ (material derivative following the solid phase). The reduced relaxation function, $g(t)$, is given by

$$g(t) = 1 + c \left[E_i \left(\frac{t}{\tau_2} \right) - E_i \left(\frac{t}{\tau_1} \right) \right] \quad (4)$$

where $E_i(\cdot)$ represents the exponential integral function, and c, τ_1, τ_2 are material properties of the QLV theory. Physically, $[1/\tau_2, 1/\tau_1]$ represents the frequency range over which most of the intrinsic viscoelastic energy dissipation occurs under dynamic loading, whereas $(1 + c \ln \tau_2/\tau_1)$ is the ratio of instantaneous to equilibrium moduli resulting from the intrinsic viscoelasticity alone. [Note that unlike the classical formulation of Fung [43], we adopt the trivial modification of the function $g(t)$ such that $g(0) = 1 + c \ln(\tau_2/\tau_1)$ and $g(\infty) = 1$, so that the viscoelastic stress $\boldsymbol{\sigma}^{ve}$ reduces to the elastic stress $\boldsymbol{\sigma}^e$ at equilibrium.] The remaining constitutive relations adopted in the current formulation are Darcy's law,

$$\mathbf{w} = -k \nabla p, \quad (5)$$

which relates the fluid flux to the pressure gradient, with k representing the hydraulic permeability (assumed isotropic and constant here, though it is generally recognized to be strain-dependent [44]), and the Conewise Linear Elasticity model of Curnier et al. [31], in its cubic symmetry embodiment [22],

$$\boldsymbol{\sigma}^e(\mathbf{E}) = \sum_{a=1}^3 \left\{ \lambda_1 [\mathbf{A}_a : \mathbf{E}] \text{tr}(\mathbf{A}_a \mathbf{E}) \mathbf{A}_a + \sum_{\substack{b=1 \\ b \neq a}}^3 \lambda_2 \text{tr}(\mathbf{A}_a \mathbf{E}) \mathbf{A}_b \right\} + 2\mu \mathbf{E}, \quad (6)$$

which describes a bimodular response, or tension-compression nonlinearity, of the solid matrix. Here, $\text{tr}(\cdot)$ is the trace operator that yields the first invariant of its tensorial argument, and $\mathbf{A}_a : \mathbf{E} = \text{tr}(\mathbf{A}_a^T \mathbf{E})$. \mathbf{A}_a is a texture tensor corresponding to each of three preferred material directions defined by the unit vectors \mathbf{a}_a ($\mathbf{a}_a \cdot \mathbf{a}_a = 1$, no sum over a , \cdot denoting the dot product of vectors), with $\mathbf{A}_a = \mathbf{a}_a \otimes \mathbf{a}_a$ (\otimes denoting the dyadic product of vectors, no sum over a). For cubic material symmetry, $\mathbf{a}_a \cdot \mathbf{a}_b = 0$ when $b \neq a$, and the three directions are generally taken to be: \mathbf{a}_1 parallel to the split line direction,² \mathbf{a}_2 perpendicular to the split line direction, and \mathbf{a}_3 normal to the articular cartilage surface. The term $\mathbf{A}_a : \mathbf{E}$ represents the component of normal strain along the preferred direction \mathbf{a}_a . Tension-compression nonlinearity stems from the conditional statement,

¹The function $g(t)$ in Eq. (3) is taken to be a scalar function for simplicity in this analysis. A most general formulation could employ a fourth-order tensor instead; for cartilage, it has sometimes been proposed to separate the viscoelastic response in bulk deformation from that in shear deformation when using an isotropic model [13,15], though this is not done here.

²Split lines have been used as indicators of predominant collagen fibril directions on the articular surface (Hulkantz, W., 1898, "Ueber die Spaltrichtungen der Gelenkknorpel," Verh. D. Anat. Ges., 12, pp. 248–256).

$$\lambda_1[\mathbf{A}_a:\mathbf{E}] = \begin{cases} \lambda_{-1}, & \mathbf{A}_a:\mathbf{E} < 0 \\ \lambda_{+1}, & \mathbf{A}_a:\mathbf{E} > 0 \end{cases} \quad (7)$$

This signifies that the material properties λ_1 differ whether the normal strain component along the direction \mathbf{a}_a is compressive or tensile. The physical meaning of these elastic constants is as follows: $H_{-A} = \lambda_{-1} + 2\mu$ is the equilibrium confined compression modulus of the tissue (the ‘‘aggregate’’ modulus) and $H_{+A} = \lambda_{+1} + 2\mu$ is the equivalent modulus in tension; λ_2 is the ‘‘off-diagonal’’ modulus, which could be determined from the equilibrium ratio of radial stress to axial strain in confined compression (the radial stress being measurable on the side wall, e.g., see the experiments of Khalsa and Eisenberg [45]). Note that the choice of an isotropic permeability is consistent with the choice of cubic symmetry for the stress–strain law, since isotropic and cubic symmetry are identical in second-order tensors such as the permeability tensor; however, it is also possible to adopt a more general orthotropic model for permeability, as in our earlier study [22].

In summary, the model presented above, which is valid for infinitesimal strains and can describe tension–compression nonlinearity [Eqs. (6) and (7)] as well as intrinsic viscoelasticity [Eqs. (3) and (4)] of the solid matrix of a solid-fluid biphasic mixture, has eight material constants: $\lambda_{-1}, \lambda_{+1}, \lambda_2, \mu, c, \tau_1, \tau_2, k$. This model can be reduced to the isotropic biphasic poroviscoelastic model of Mak [13] by letting $\lambda_{-1} = \lambda_{+1} = \lambda_2 = \lambda$ (and noting that $\mathbf{A}_1 + \mathbf{A}_2 + \mathbf{A}_3 = \mathbf{I}$). It can be reduced to our recently proposed biphasic-CLE model [22] by letting $c = 0$. It can also be reduced to the linear isotropic biphasic theory of Mow et al. [1] by implementing both of the reductions described above.

Uniaxial Tension and Unconfined Compression

Typical experiments of unconfined compression of articular cartilage are performed on cylindrical samples (e.g., 1 mm thick, 6 mm in diameter), which can be easily harvested with a circular core punch cutting perpendicularly to the articular surface (e.g., [1]). In contrast, uniaxial tensile tests are performed on long strips of cartilage, either dumbbell shaped or prismatic (e.g., 10 mm long), with a rectangular cross section (e.g., 0.2×1.5 mm), which are typically harvested with a pair of blades perpendicularly to the surface (e.g., [33,35]). The solution of Armstrong et al. [30] for unconfined compression of a linear isotropic biphasic material, as well as many subsequent solutions (e.g., [7,8]) assumed frictionless conditions at the loading platens, which is reasonable in view of the typically low friction coefficient of articular cartilage. This simplification, along with the assumption of axisymmetric conditions facilitated by the specimen geometry, leads to equations amenable to a closed-form analytical solution. In contrast, the biphasic or biphasic poroviscoelastic analysis of the uniaxial tensile response of cartilage has generally been performed on prismatic bars with rectangular cross sections, requiring either a simplification of the boundary conditions [46] or a numerical scheme such as finite element analysis [47]; the reason is that the analysis of the biphasic response of a prismatic bar with rectangular cross section, whose lateral boundaries are free draining, is fully three dimensional and does not lend itself to an analytical closed-form solution because of the complexity of the transient interstitial fluid flow fields that would result from loading. Therefore, in order to achieve a closed-form solution for the biphasic-CLE-QLV analysis of uniaxial tension for the purpose of examining the different

responses of cartilage in tension and compression, we assume in this study that the cartilage specimen is a prismatic bar with a circular cross section, while recognizing that such a specimen geometry cannot be easily obtained in practice by typical specimen preparation. It will be demonstrated below that this assumption is not as restrictive as it first may seem. By St. Venant’s principle, the effects of the clamping conditions at the two ends of the prismatic bar are also neglected, since the specimen length is typically much greater than its characteristic cross-sectional width, so that the analyses of uniaxial tension and unconfined compression are treated in a similar fashion, with the only difference in those two configurations arising from the bimodular constitutive assumptions of the CLE theory.

The reduction of the general biphasic equations to the configuration of unconfined compression with frictionless platens and axisymmetric conditions has been described previously for the linear isotropic biphasic model [30], the poroviscoelastic biphasic model [21], and the biphasic-CLE model [22]. In these analyses, the shear traction at the interface between cartilage and the loading platens is set to zero and the axial normal strain is homogeneous; the interstitial fluid pressure and normal traction are also set to zero on the lateral boundary. The same approach can be followed with the constitutive equations of Eqs. (3)–(6), hence only a summary of the results is presented here. As is typical for this type of problems, the governing equations and closed-form solution is given in Laplace transform space. The differential equation for the radial displacement is given by

$$\frac{\partial^2 \bar{u}_r}{\partial r^2} + \frac{1}{r} \frac{\partial \bar{u}_r}{\partial r} - \frac{\bar{u}_r}{r^2} - f^\pm \bar{u}_r = \frac{r f^\pm}{2} \bar{\varepsilon}(s), \quad (8)$$

whereas the boundary conditions reduce to

$$\bar{u}_r|_{r=0} = 0, \quad H_{\mp A} \frac{\partial \bar{u}_r}{\partial r} + \lambda_2 \left(\frac{\bar{u}_r}{r} + \bar{\varepsilon}(s) \right) \Big|_{r=r_0} = 0. \quad (9)$$

The fluid pressure can be determined from the radial displacement using

$$\bar{p}(r,s) = -\frac{1}{k} \int_r^{r_0} [s \bar{u}_r(\rho,s) + s \rho \bar{\varepsilon}(s)/2] d\rho. \quad (10)$$

The solution then reduces to

$$\bar{u}_r^\pm(r,s) = \frac{r_0}{2} \left[\frac{\left(1 - \frac{\lambda_2}{H_{\mp A}}\right) I_1\left(\sqrt{f^\pm} \frac{r}{r_0}\right)}{\sqrt{f^\pm} I_0(\sqrt{f^\pm}) - \left(1 - \frac{\lambda_2}{H_{\mp A}}\right) I_1(\sqrt{f^\pm})} - \frac{r}{r_0} \right] \bar{\varepsilon}^\pm(s), \quad (11)$$

$$\bar{p}^\pm(r,s) = \frac{H_{\mp A}}{2} \left(1 + c \ln \frac{1 + \tau_2 s}{1 + \tau_1 s}\right) \times \left\{ \frac{\sqrt{f^\pm} \left(1 - \frac{\lambda_2}{H_{\mp A}}\right) \left[I_0\left(\sqrt{f^\pm} \frac{r}{r_0}\right) - I_0(\sqrt{f^\pm}) \right]}{\sqrt{f^\pm} I_0(\sqrt{f^\pm}) - \left(1 - \frac{\lambda_2}{H_{\mp A}}\right) I_1(\sqrt{f^\pm})} \right\} \bar{\varepsilon}^\pm(s), \quad (12)$$

$$\bar{F}^\pm(s) = H_{\mp A} \left(1 + c \ln \frac{1 + \tau_2 s}{1 + \tau_1 s}\right) \left\{ \frac{\left(\frac{2H_{\mp A} - 3\lambda_2 + H_{\mp A}}{2H_{\mp A}}\right) \sqrt{f^\pm} I_0(\sqrt{f^\pm}) + \left(1 - \frac{\lambda_2}{H_{\mp A}}\right) \left(\frac{2\lambda_2 - H_{\mp A} - H_{\mp A}}{H_{\mp A}}\right) I_1(\sqrt{f^\pm})}{\sqrt{f^\pm} I_0(\sqrt{f^\pm}) - \left(1 - \frac{\lambda_2}{H_{\mp A}}\right) I_1(\sqrt{f^\pm})} \right\} \bar{\varepsilon}^\pm(s), \quad (13)$$

$$\frac{\bar{F}_p^\pm(s)}{\pi r_0^2} = H_{\mp A} \left(1 + c \ln \frac{1 + \tau_2 s}{1 + \tau_1 s} \right) \times \left\{ \frac{\left(1 - \frac{\lambda_2}{H_{\mp A}} \right) \left[I_1(\sqrt{f^\pm}) - \frac{1}{2} \sqrt{f^\pm} I_0(\sqrt{f^\pm}) \right]}{\sqrt{f^\pm} I_0(\sqrt{f^\pm}) - \left(1 - \frac{\lambda_2}{H_{\mp A}} \right) I_1(\sqrt{f^\pm})} \right\} \bar{\varepsilon}^\pm(s), \quad (14)$$

where

$$f^\pm = \frac{r_0^2 s}{H_{\mp A} k \left(1 + c \ln \frac{1 + \tau_2 s}{1 + \tau_1 s} \right)}. \quad (15)$$

In these equations, r is the radial coordinate, u_r refers to the radial displacement, p is the interstitial fluid pressure, ε is the axial strain, F is the total axial force across the specimen, and F_p is that component of the force supported by interstitial fluid pressure, i.e., $F_p = 2\pi \int_0^{r_0} r p dr$, where r_0 is the specimen radius. $I_0(\cdot)$ and $I_1(\cdot)$ are modified Bessel functions of the first kind, of order 0 and 1, respectively. Overbars indicate Laplace transformation from the time domain and s is the Laplace transform variable. Superscripted \pm on these parameters refer to the solution for tension (+) or compression (-), as it can be observed that these solutions differ by the interchange of the material constants $H_{+A} = \lambda_{+1} + 2\mu$ and $H_{-A} = \lambda_{-1} + 2\mu$. Note that the solution does not depend on the axial dimension (thickness or length) of the cylindrical specimen.

These solutions are valid for a variety of loading conditions. For example, for a step application of strain with a magnitude ε_0 , use $\bar{\varepsilon}^\pm(s) = \pm \varepsilon_0/s$; if the strain is ramped over a ramp time of t_0 and subsequently kept constant at a magnitude of ε_0 , use $\bar{\varepsilon}^\pm(s) = \pm (1 - e^{-st_0})\varepsilon_0/s^2 t_0$. Alternatively, the total axial load $\bar{F}^\pm(s)$ may be prescribed in a similar way, and a solution for $\bar{\varepsilon}^\pm(s)$ obtained from Eq. (13) then substituted into the remaining expressions.

For step or ramp strain application, inverse Laplace transformation into the time domain can be performed numerically, e.g., using the INLAP routine from the IMSL library (Visual Numerics, Inc., Houston, TX).³ For the steady-state solution to a sinusoidal axial load or strain, it suffices to substitute $s = i\omega$ into the solutions of Eqs. (11)–(15), where ω is the angular frequency of the applied load or strain and $i = \sqrt{-1}$, to derive the frequency-dependent amplitude and phase response of the corresponding parameter.

The dynamic modulus $\bar{G}^\pm(s)$ of this biphasic-CLE-QLV material can be derived from the ratio of $\bar{F}^\pm(s)/\pi r_0^2$ and $\bar{\varepsilon}^\pm(s)$ in Eq. (13). To determine the material's "instantaneous" modulus (or the modulus in the limit of loading at high frequency), denoted by $E_{\pm Y}^{0+}$, it suffices to take the limit of the resulting expression as $s \rightarrow \infty$, which corresponds to the real time limit of $t \rightarrow 0^+$:

$$E_{\pm Y}^{0+} = \left(1 + c \ln \frac{\tau_2}{\tau_1} \right) \left(H_{\pm A} - \frac{3}{2} \lambda_2 + \frac{H_{\mp A}}{2} \right). \quad (16)$$

Similarly, the modulus at equilibrium (or in the limit of loading at very low frequency), $E_{\pm Y}$ (Young's modulus in classical elasticity), can be obtained by taking the limit of the dynamic modulus as $s \rightarrow 0$,

$$E_{\pm Y} = H_{\pm A} - \frac{2\lambda_2^2}{H_{\mp A} + \lambda_2}. \quad (17)$$

It can be observed that, as expected, the equilibrium modulus is independent of the QLV parameters. Finally, the instantaneous (or high-frequency) fluid load support can be obtained by taking the limit, as $s \rightarrow \infty$, of the ratio of the expressions in Eqs. (14) and (13),

$$-\frac{\bar{F}_p^\pm}{\bar{F}^\pm} = \frac{1}{1 + 2 \frac{H_{\pm A} - \lambda_2}{H_{\mp A} - \lambda_2}}. \quad (18)$$

It is noteworthy that this expression is independent of the QLV parameters, even though it represents an instantaneous response.

Results

A variety of testing configurations in tension and compression can be simulated from the solutions described above, a subset of which are presented here to provide sufficient insight into the behavior of this biphasic-CLE-QLV model. Since this compound model has not been employed previously in the literature, representative material properties used in the simulations here derive from two separate sources: For the biphasic-CLE properties, we employ the results of our recent analysis [22], derived from confined and unconfined compression stress-relaxation and torsional shear experiments on bovine articular cartilage; $H_{+A} = 13.2$ MPa, $H_{-A} = 0.64$ MPa, $\lambda_2 = 0.48$ MPa, $\mu = 0.17$ MPa, $k = 6.1 \times 10^{-16}$ m⁴/N.s; these properties were obtained under a total strain of approximately 18 percent (including tare loading). For the QLV parameters, we use the results of Setton et al. [14] who curve-fit the biphasic poroviscoelastic theory of Mak [13] to confined compression creep data, also on bovine articular cartilage: $c = 0.16$, $\tau_1 = 0.06$ s, $\tau_2 = 201$ s.

In uniaxial tension, a representative radius of $r_0 = 0.345$ mm is employed, which produces a surface area equivalent to a rectangular cross section of dimensions 1.5 mm \times 0.25 mm. In the first analysis, a step tensile strain of magnitude $\varepsilon_0 = 0.10$ (10 percent) is applied to the sample and the time-dependent stress-relaxation response of the biphasic-CLE-QLV model is presented in Fig. 1, together with the specialized case of the biphasic-CLE model (with $c = 0$). It can be noted that, unlike the biphasic-CLE-QLV response, the biphasic-CLE response exhibits almost no transient relaxation under this testing configuration. Substitution of these material constants into Eq. (16) confirms that the instantaneous tensile modulus of the biphasic-CLE-QLV material, E_{+Y}^{0+}

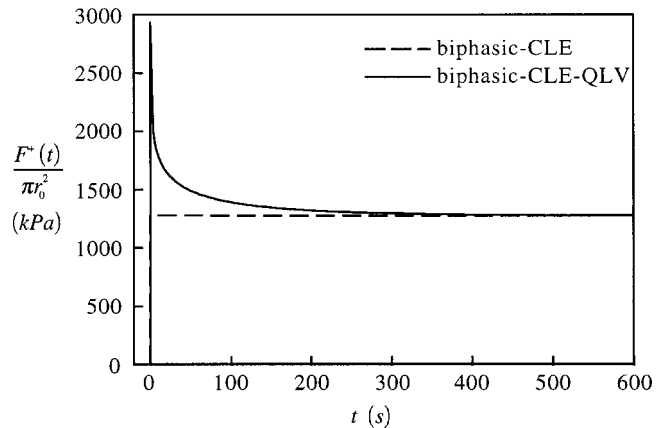


Fig. 1 Uniaxial tensile response of the biphasic-CLE-QLV and biphasic-CLE models, to a step strain of $\varepsilon_0 = 0.10$ (10 percent), as derived from Eq. (13) by numerical inverse Laplace transformation

³Numerical inverse Laplace transformation is best achieved by nondimensionalizing the expressions in Eqs. (6)–(12) to avoid numerical overflow or underflow. Though IMSL has a built-in routine to evaluate Bessel functions with a complex argument, a custom-written routine implementing asymptotic expansions for large arguments was employed instead.

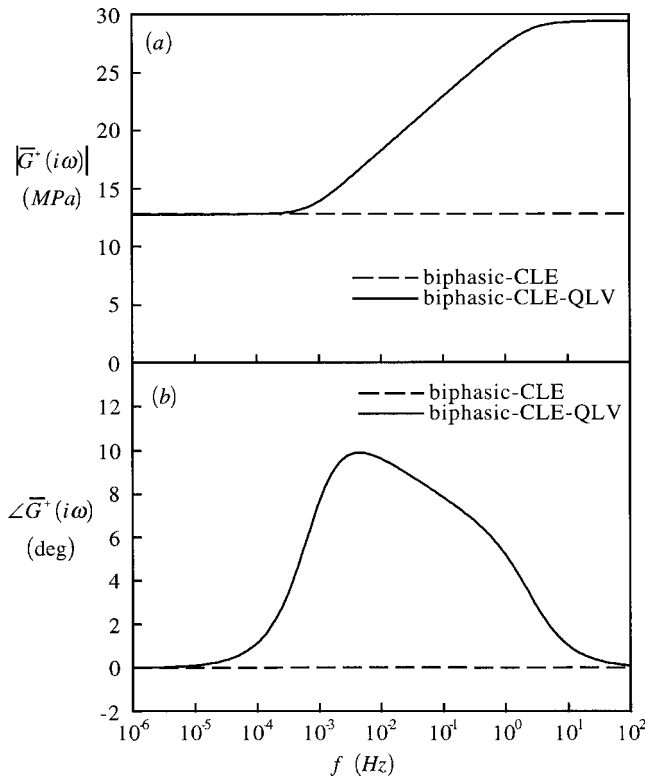


Fig. 2 Dynamic modulus versus frequency under uniaxial tensile loading, for the biphasic-CLE-QLV and biphasic-CLE models: (a) magnitude; (b) phase angle. In the limit of high frequencies, the magnitude of the dynamic modulus is given by E_{+Y}^{0+} in Eq. (16), whereas at low frequencies it is given by E_{+Y} in Eq. (17)

=29.4 MPa, is considerably greater than that of the biphasic-CLE material, $E_{+Y}^{0+}=12.8$ MPa. In contrast, for both models, the equilibrium modulus in tension is $E_{+Y}=12.3$ MPa. The dynamic modulus in tension is displayed for both models in Fig. 2, which displays the amplitude and phase angle as a function of frequency over the range $f = \omega/2\pi = 10^{-6} - 10^2$ Hz. For reference, the three characteristic frequencies for the material are $f_+ = H_{-A}k/r_0^2 = 0.0033$ Hz, $1/\tau_2 = 0.005$ Hz, $1/\tau_1 = 16.7$ Hz. As already evidenced by the values of E_{+Y}^{0+} and E_{+Y} , there is virtually no frequency dependence of the dynamic tensile modulus in the biphasic-CLE model, whereas the inclusion of QLV produces a characteristic flow-independent viscoelastic response.

In unconfined compression, a radius of $r_0 = 2.39$ mm is assumed.⁴ In the first of these analyses, a ramped-strain stress-relaxation test is employed, with $\epsilon_0 = 0.10$ and $t_0 = 3$ s, 150 s, and 300 s. The resulting stress-relaxation responses are presented in Fig. 3, with and without QLV effects. Unlike the case for tension, a very significant transient response is observed in unconfined compression in both models. Differences in the two models are most evident only in the fastest of the ramp rates employed ($t_0 = 3$ s), with the peak stress at the end of the ramp achieving a larger value for the biphasic-CLE-QLV model. The amplitude and phase angle of the unconfined compression dynamic modulus is presented in Fig. 4, for both models; for this testing configuration, the three characteristic frequencies for the material are $f_- = H_{+A}k/r_0^2 = 0.0014$ Hz, $1/\tau_2 = 0.005$ Hz, $1/\tau_1 = 16.7$ Hz. From this figure, as from Eq. (16), it can be observed that E_{-Y}^{0+}

⁴Representative radii are not required when performing these analyses with the nondimensional form of the equations; they are used here for illustration.

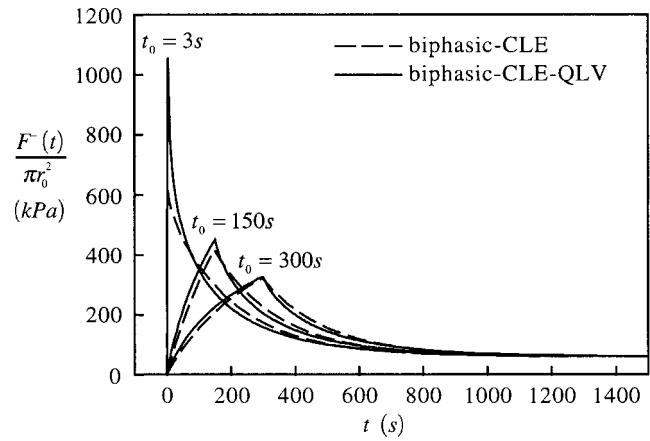


Fig. 3 Unconfined compression stress-relaxation response of the biphasic-CLE-QLV and biphasic-CLE models, to a ramp strain of magnitude $\epsilon_0 = 0.10$ (10 percent), and for three different ramp times ($t_0 = 3$ s, 150 s, and 300 s), as derived from Eq. (13) by numerical inverse Laplace transformation

=15.0 MPa for the biphasic-CLE-QLV model, and $E_{-Y}^{0+} = 6.5$ MPa for the biphasic-CLE model, whereas the equilibrium compressive modulus is only $E_{-Y} = 0.57$ MPa for both cases.

Discussion

The short-term objective of this study was to investigate the role of intrinsic viscoelasticity of the solid matrix of cartilage

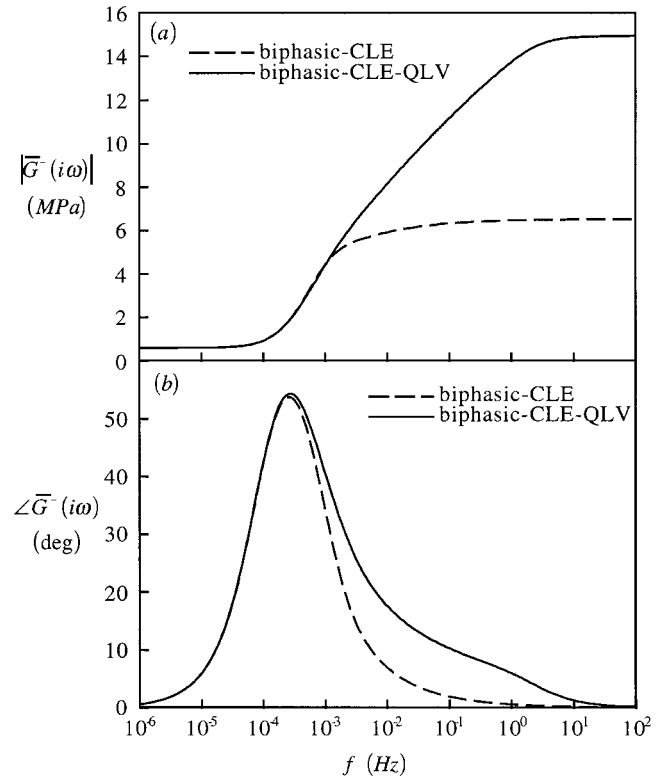


Fig. 4 Dynamic modulus versus frequency under unconfined compression loading, for the biphasic-CLE-QLV and biphasic-CLE models: (a) magnitude; (b) phase angle. In the limit of high frequencies the magnitude of the dynamic modulus is given by E_{-Y}^{0+} in Eq. (16), whereas at low frequencies it is given by E_{-Y} in Eq. (17)

within the context of a biphasic mixture theory that accounts for tension–compression nonlinearity. The long-term objectives are to help elucidate the mechanism by which articular cartilage can sustain typical physiological stresses in the range of 2–6 MPa (e.g., [41,42]), with occasional peak values as high as 18 MPa [48], while exhibiting a compressive equilibrium modulus on the order of 0.5 MPa only; and to provide a theoretical framework that can simultaneously predict the tensile and compressive responses of articular cartilage, under transient and dynamic conditions. As discussed below, the results of this study provide a more comprehensive agreement between theory and experiments in the literature, than achieved from the linear biphasic, the QLV, the biphasic-QLV (biphasic poroviscoelastic), or the biphasic-CLE theories alone.

First, because the biphasic-CLE-QLV subsumes the linear biphasic theory, it can provide the same successful agreement with confined compression experiments as demonstrated previously (e.g., [1,2,18,29,49]). Second, because the biphasic-QLV and the biphasic-CLE are subsumed by the more general model, good agreement can also be expected in the curvefitting of unconfined compression stress-relaxation results [17,22]. However, under dynamic unconfined compression, cartilage has been shown to exhibit a dynamic compressive modulus on the order of 12–20 MPa [50,51] at the highest tested frequencies. Looking at Eq. (16) with $c=0$, the highest achievable dynamic modulus with the biphasic-CLE model is $E_{-y}^{0+} \approx H_{+A}/2$ (given that $H_{-A}, \lambda_2 \ll H_{+A}$), which puts it on the order of 6.5 MPa when using the representative value of H_{+A} employed in the simulations given above (see the high-frequency range in Fig. 4). With the biphasic-QLV (i.e., letting $H_{+A}=H_{-A}$ in Eq. (16)), the highest predicted dynamic modulus in compression would be $E_{-y}^{0+} = (3/2)(1+c \ln \tau_2/\tau_1)(H_{-A}-\lambda_2)$, which is on the order of 0.5 MPa for the typical material constants used above. Clearly, while the biphasic-CLE model is a better predictor of the dynamic unconfined compression modulus than the biphasic-QLV, it still falls somewhat short of the values observed experimentally. However, when using the combined biphasic-CLE-QLV model, Eq. (16) produces a dynamic unconfined compression modulus E_{-y}^{0+} on the order of 15 MPa (Fig. 4), in better agreement with experiments in the literature.

Looking at Eq. (17), it can be observed that the biphasic-CLE theory can account for the differences observed in the literature between the compressive and tensile equilibrium moduli of cartilage (e.g., $E_{-y} = 0.55$ MPa and $E_{+y} = 12.3$ MPa, using the above-given typical material constants), represented for typical samples of humeral head cartilage in Fig. 5; clearly, neither the linear biphasic nor the biphasic-QLV models account for tension–compression nonlinearity, so they are unable to model both tension and compression using consistent material constants. However, as observed in Fig. 1, the biphasic-CLE is unable to produce a substantial transient response under a step strain in tension, even though such responses have always been observed in the literature (e.g., [35,37,40], also see the typical experimental response in Fig. 6), whereas the biphasic-CLE-QLV can account for this effect. It is important to appreciate that in tension, the flow-dependent viscoelasticity is curtailed by the large difference between the tensile and compressive moduli in the biphasic-CLE and biphasic-CLE-QLV theories, whereas in compression, the fluid pressurization is enhanced by the tension–compression nonlinearity. This is evident from the fluid load support as given in Eq. (18); whereas in unconfined compression the fluid load support for the biphasic-CLE or biphasic-CLE-QLV models is very high ($|\bar{F}_p^-/\bar{F}^-| = 97.6$ percent), it becomes virtually negligible in tension ($|\bar{F}_p^+/\bar{F}^+| = 0.6$ percent). For the linear biphasic or the biphasic-QLV, the fluid load support in tension and compression remains the same, $|\bar{F}_p^\pm/\bar{F}^\pm| = 33.3$ percent; indeed, the latter theories would predict the same transient relaxation in tension as

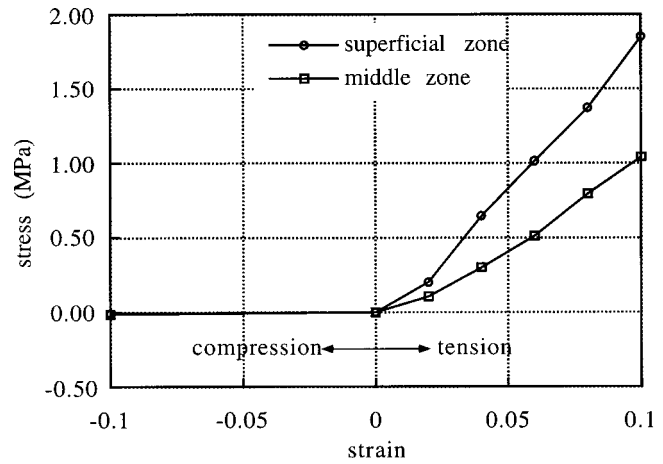


Fig. 5 Typical experimental equilibrium tensile and compressive responses of human humeral head articular cartilage from the superficial-CLE and middle zones (55 y.o. male). The tensile response is measured from long prismatic samples with rectangular cross section, harvested parallel to the surface, along the split line direction; the compressive response is measured from cylindrical plugs harvested normal to the articular surface [34].

in unconfined compression, though they otherwise appear to be unsuitable for predicting the tension–compression nonlinearity as discussed above.

Since flow-dependent viscoelasticity is negligible when $H_{-A}/H_{+A} \ll 1$, uniaxial tension experiments may conceivably be used to extract only the QLV parameters, c , τ_1 , τ_2 , and the equilibrium tensile modulus, E_{+y} , even when using the framework of the biphasic-CLE-QLV theory. This simplification in the analysis of experimental data in uniaxial tension also implies that the precise geometry of the specimen cross section would not impact the experimental outcome since fluid flow effects, which otherwise depend on geometry, are negligible. The results of this analysis also suggest that for biological hydrated soft tissues, which generally sustain very little compressive loads and thus exhibit very significant tension–compression nonlinearity, such as tendons and ligaments, flow-dependent viscoelasticity may not be a significant effect.

The results of this study are primarily based on a theoretical analysis at this time, though favorable qualitative comparisons are observed relative to literature findings. Experiments that directly

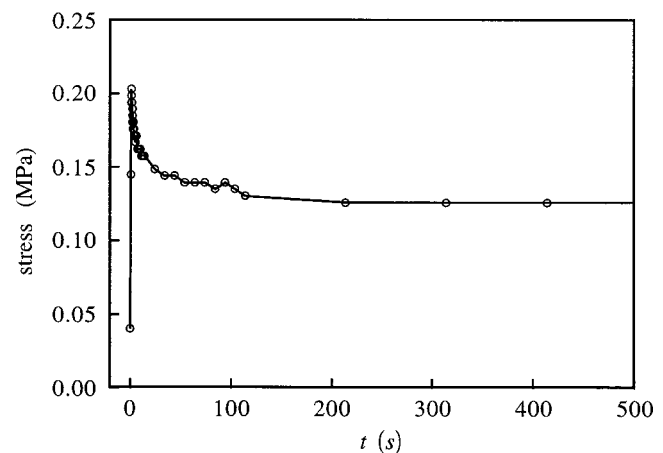


Fig. 6 Experimental uniaxial tensile response of the superficial zone specimen of Fig. 5 to a ramp strain of $\epsilon_0=0.02$ (2 percent) and ramp time of $t_0=1$ s, as a function of time

test the predictions of the biphasic-CLE-QLV model represent the next step in this effort to establish a more comprehensive theoretical framework for articular cartilage. Recently, models that have accounted for the tension-compression nonlinearity of cartilage [7,22], such as the biphasic-CLE model reviewed above, have demonstrated that interstitial fluid load support is considerably enhanced in compression by the disparity in tensile and compressive moduli of cartilage, producing a greater dynamic modulus. The current study demonstrates that the addition of intrinsic viscoelasticity provides the necessary boost to the theoretical prediction of the dynamic modulus to match experimental findings at higher frequencies. In the biphasic-CLE-QLV model adopted in this study, the dynamic modulus is greater than that of the biphasic-CLE model by a factor of $(1 + c \ln \tau_2/\tau_1)$ according to Eq. (16). Interestingly, in this model, the incorporation of solid matrix intrinsic viscoelasticity neither enhances nor defeats the fluid load support, as indicated by Eq. (18). As noted by others [17], and evidenced by comparing the biphasic-CLE and biphasic-CLE-QLV results of Fig. 3 or 4, it appears that the effect of intrinsic solid matrix viscoelasticity is most evident at relatively fast strain rates (e.g., with a ramp time of $t_0 = 3$ s in Fig. 3 in stress-relaxation, or at dynamic frequencies above 10^{-3} Hz according to Fig. 4); the stress-relaxation results of Fig. 3 suggest that a combination of stress-relaxation experiments with a slow ramp time and a fast ramp time could also be used to discriminate between flow-dependent and flow-independent effects (see a typical experimental response in Fig. 7), though not as dramatically as uniaxial tensile tests (Fig. 1 or Fig. 6).

There are a number of limitations to the current study. For example, the assumption of a linear response in tension is known to be a simplification, since cartilage has been shown to behave nonlinearly even at small tensile strains; furthermore, the current model does not adequately describe the anisotropy of cartilage, such as the known disparity in tensile moduli measured parallel and perpendicular to the split lines, as well as the observation of tensile Poisson's ratios in excess of 0.5, though these could be potentially addressed using an orthotropic model. The known inhomogeneity of cartilage properties from the surface to the deep zone would need to be taken into account to produce more accurate results. A finite strain formulation of the constitutive equations would also be more appropriate to investigate higher physiological loads. These issues, which typically increase the complexity of cartilage modeling, can be addressed in future analyses.

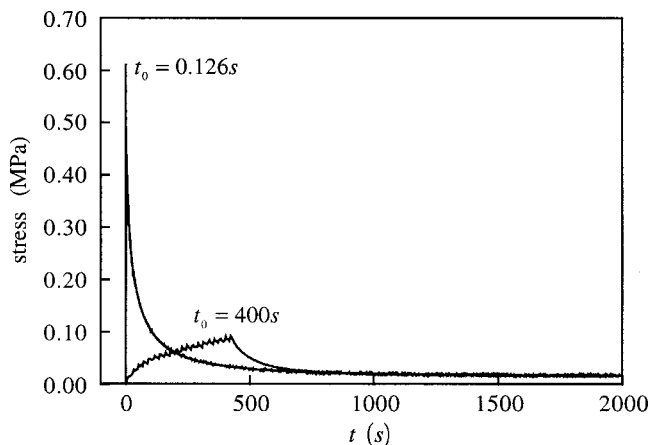


Fig. 7 Typical experimental unconfined compression stress-relaxation response of bovine glenohumeral articular cartilage, to a ramp strain of magnitude $\epsilon_0 = 0.05$ (5 percent), and for two different ramp times ($t_0 = 0.126$ s and $t_0 = 400$ s)

Conclusion

This study attempts to explain various observed experimental findings in the testing of articular cartilage, by combining several constitutive models previously described in the literature, each of which had demonstrated success in one or more testing configurations. By comparing theoretical predictions with experimental findings in the literature, it is found that a simultaneous prediction of compression and tension experiments, under stress-relaxation and dynamic loading, can be achieved when taking into account flow-dependent and flow-independent viscoelasticity effects, as well as tension-compression nonlinearity. While a guiding principle of constitutive modeling of biological tissues is to adopt the simplest possible formulation that can describe experimental data, it is becoming increasingly clear that the complexity of articular cartilage mechanics requires more elaborate models than those already presented in the literature. The biphasic-CLE-QLV model adopted in this study has the advantage that it employs as building blocks theories that have proved popular and are thus familiar to the concerned research community. In the embodiment adopted here, the model has eight material constants; clearly, this signifies that an experimental characterization of the material properties of a particular tissue sample could not come from a single test but would rather require multiple experiments, either on the same sample or on adjoining samples from the same tissue source. The combination of tests that might provide sufficient data to determine these constants uniquely is the subject of ongoing studies.

Acknowledgments

This study was supported in part by the National Institute for Arthritis, and Musculoskeletal and Skin Diseases of the National Institutes of Health (AR46532, AR43628, AR42850, and AR41913).

References

- [1] Mow, V. C., Kuei, S. C., Lai, W. M., and Armstrong, C. G., 1980, "Biphasic Creep and Stress Relaxation of Articular Cartilage in Compression: Theory and Experiments," *ASME J. Biomech. Eng.*, **102**, pp. 73–84.
- [2] Frank, E. H., and Grodzinsky, A. J., 1987, "Cartilage Electromechanics—II. A Continuum Model of Cartilage Electrokinetics and Correlation With Experiments," *J. Biomech.*, **20**, pp. 629–639.
- [3] Lai, W. M., Hou, J. S., and Mow, V. C., 1991, "A Triphasic Theory for the Swelling and Deformation Behaviors of Articular Cartilage," *ASME J. Biomech. Eng.*, **113**, pp. 245–258.
- [4] Ateshian, G. A., Warden, W. H., Kim, J. J., Grelsamer, R. P., and Mow, V. C., 1997, "Finite Deformation Biphasic Material Properties of Bovine Articular Cartilage From Confined Compression Experiments," *J. Biomech.*, **30**, pp. 1157–1164.
- [5] Huyghe, J. M., and Janssen, J. D., 1997, "Quadruphase Mechanics of Swelling Incompressible Porous Media," *Int. J. Eng. Sci.*, **35**, pp. 793–802.
- [6] Gu, W. Y., Lai, W. M., and Mow, V. C., 1998, "A Mixture Theory for Charged Hydrated Soft Tissues Containing Multi-electrolytes: Passive Transport and Swelling Behaviors," *ASME J. Biomech. Eng.*, **120**, pp. 169–180.
- [7] Soulhat, J., Buschmann, M. D., and Shirazi-Adl, A., 1999, "A Fibril-Network Reinforced Model of Cartilage in Unconfined Compression," *ASME J. Biomech. Eng.*, **121**, pp. 340–347.
- [8] Cohen, B., Lai, W. M., and Mow, V. C., 1998, "A Transversely Isotropic Biphasic Model for Unconfined Compression of Growth Plate and Chondroepiphysis," *ASME J. Biomech. Eng.*, **120**, pp. 491–496.
- [9] Cohen, B., Gardner, T. R., and Ateshian, G. A., 1993, "The Influence of Transverse Isotropy on Cartilage Indentation Behavior—A Study of the Human Humeral Head," *Trans. Orthop. Res. Soc.*, **18**, p. 185.
- [10] Mow, V. C., Good, P. M., and Gardner, T. R., 2000, "A New Method to Determine the Tensile Properties of Articular Cartilage Using the Indentation Test," *Trans. Orthop. Res. Soc.*, **25**, p. 103.
- [11] Hayes, W. C., and Mockros, L. F., 1971, "Viscoelastic Properties of Human Articular Cartilage," *J. Appl. Physiol.*, **31**, pp. 562–568.
- [12] Hayes, W. C., and Bodine, A. J., 1978, "Flow-Independent Viscoelastic Properties of Articular Cartilage Matrix," *J. Biomech.*, **11**, pp. 407–419.
- [13] Mak, A. F., 1986, "The Apparent Viscoelastic Behavior of Articular Cartilage—The Contributions From the Intrinsic Matrix Viscoelasticity and Interstitial Fluid Flows," *ASME J. Biomech. Eng.*, **108**, pp. 123–130.
- [14] Setton, L. A., Zhu, W., and Mow, V. C., 1993, "The Biphasic Poroviscoelastic Behavior of Articular Cartilage: Role of the Surface Zone in Governing the Compressive Behavior," *J. Biomech.*, **26**, pp. 581–592.
- [15] Suh, J.-K., and DiSilvestro, M. R., 1999, "Biphasic Poroviscoelastic Behavior of Hydrated Biological Soft Tissue," *ASME J. Appl. Mech.*, **66**, pp. 528–535.

- [16] Suh, J.-K., and Bai, S., 1997, "Biphasic Poroviscoelastic Behavior of Articular Cartilage in Creep Indentation Test," *Trans. Orthop. Res. Soc.*, **22**, p. 823.
- [17] DiSilvestro, M. R., Zhu, Q., and Suh, J.-K., 1999, "Biphasic Poroviscoelastic Theory Predicts the Strain Rate Dependent Viscoelastic Behavior of Articular Cartilage," *Proc. 1999 Bioeng. Conf.*, ASME BED-Vol. 42, pp. 105–106.
- [18] Soltz, M. A., and Ateshian, G. A., 2000, "Interstitial Fluid Pressurization During Confined Compression Cyclical Loading of Articular Cartilage," *Ann. Biomed. Eng.*, **28**, pp. 150–159.
- [19] Zhu, W., Mow, V. C., Koob, T. J., and Eyre, D. R., 1993, "Viscoelastic Shear Properties of Articular Cartilage and the Effects of Glycosidase Treatments," *J. Orthop. Res.*, **11**, pp. 771–781.
- [20] Setton, L. A., Mow, V. C., and Howell, D. S., 1995, "Mechanical Behavior of Articular Cartilage in Shear Is Altered by Transection of the Anterior Cruciate Ligament," *J. Orthop. Res.*, **13**, pp. 473–482.
- [21] Mak, A. F., 1986, "Unconfined Compression of Hydrated Viscoelastic Tissues: A Biphasic Poroviscoelastic Analysis," *Biorheology*, **23**, pp. 371–383.
- [22] Soltz, M. A., and Ateshian, G. A., 2000, "A Conewise Linear Elasticity Mixture Model for the Analysis of Tension-Compression Nonlinearity in Articular Cartilage," *ASME J. Biomech. Eng.*, **122**, pp. 576–586.
- [23] Guilak, F., Ratcliffe, A., and Mow, V. C., 1995, "Chondrocyte Deformation and Local Tissue Strain in Articular Cartilage: A Confocal Microscopy Study," *J. Orthop. Res.*, **13**, pp. 410–421.
- [24] Schinagl, R. M., Gurskis, D., Chen, A. C., and Sah, R. L., 1997, "Depth-Dependent Confined Compression Modulus of Full-Thickness Bovine Articular Cartilage," *J. Orthop. Res.*, **15**, pp. 499–506.
- [25] Wang, C. C.-B., Soltz, M. A., Mauck, R. L., Valhmu, W. B., Ateshian, G. A., and Hung, C. T., 2000, "Comparison of Equilibrium Axial Strain Distribution in Articular Cartilage Explants and Cell-Seeded Alginate Disks Under Unconfined Compression," *Trans. Orthop. Res. Soc.*, **25**, p. 131.
- [26] Wang, C. C.-B., Hung, C. T., and Mow, V. C., 2001, "An Analysis of the Effects of Depth-Dependent Aggregate Modulus on Articular Cartilage Stress-Relaxation Behavior in Compression," *J. Biomech.*, **34**, pp. 75–84.
- [27] Li, L. P., Buschmann, M. D., and Shirazi-Adl, A., 2000, "A Fibril Reinforced Nonhomogeneous Poroelastic Model for Articular Cartilage: Inhomogeneous Response in Unconfined Compression," *J. Biomech.*, **33**, pp. 1533–1541.
- [28] Holmes, M. H., and Mow, V. C., 1990, "The Nonlinear Characteristics of Soft Gels and Hydrated Connective Tissues in Ultrafiltration," *J. Biomech.*, **23**, pp. 1145–1156.
- [29] Soltz, M. A., and Ateshian, G. A., 1998, "Experimental Verification and Theoretical Prediction of Cartilage Interstitial Fluid Pressurization at an Impermeable Contact Interface in Confined Compression," *J. Biomech.*, **31**, pp. 927–934.
- [30] Armstrong, C. G., Mow, V. C., and Lai, W. M., 1984, "An Analysis of Unconfined Compression of Articular Cartilage," *ASME J. Biomech. Eng.*, **106**, pp. 165–173.
- [31] Curnier, A., He, Q.-C., and Zysset, P., 1995, "Conewise Linear Elastic Materials," *J. Elast.*, **37**, pp. 1–38.
- [32] Kempson, G. E., Freeman, M. A., and Swanson, S. A., 1968, "Tensile Properties of Articular Cartilage," *Nature (London)*, **220**, pp. 1127–1128.
- [33] Woo, S. L.-Y., Akeson, W. H., and Jemcott, G. F., 1976, "Measurements of Nonhomogeneous, Directional Mechanical Properties of Articular Cartilage in Tension," *J. Biomech.*, **9**, pp. 785–791.
- [34] Armstrong, C. G., and Mow, V. C., 1982, "Variations in the Intrinsic Mechanical Properties of Human Articular Cartilage With Age, Degeneration, and Water Content," *J. Bone Jt. Surg., Am. Vol.*, **64A**, pp. 88–94.
- [35] Akizuki, S., Mow, V. C., Muller, F., Pita, J. C., Howell, D. S., and Manicourt, D. H., 1986, "Tensile Properties of Human Knee Joint Cartilage: I. Influence of Ionic Conditions, Weight Bearing, and Fibrillation on the Tensile Modulus," *J. Orthop. Res.*, **4**, pp. 379–392.
- [36] Akizuki, S., Mow, V. C., Muller, F., Pita, J. C., and Howell, D. S., 1987, "Tensile Properties of Human Knee Joint Cartilage. II. Correlations Between Weight Bearing and Tissue Pathology and the Kinetics of Swelling," *J. Orthop. Res.*, **5**, pp. 173–186.
- [37] Schmidt, M. B., Mow, V. C., Chun, L. E., and Eyre, D. R., 1990, "Effects of Proteoglycan Extraction on the Tensile Behavior of Articular Cartilage," *J. Orthop. Res.*, **8**, pp. 353–363.
- [38] Huang, C.-Y., Stankiewicz, A., Ateshian, G. A., Flatow, E. L., Bigliani, L. U., and Mow, V. C., 1999, "Tensile and Compressive Stiffness of Human Glenohumeral Cartilage Under Finite Deformation," *Proc. 1999 Bioeng. Conf.*, ASME BED-Vol. 42, pp. 469–470.
- [39] Soltz, M. A., Palma, C., Barsoumian, S., Wang, C. C.-B., Hung, C. T., and Ateshian, G. A., 2000, "Multi-Axial Loading of Bovine Articular Cartilage in Unconfined Compression," *Trans. Orthop. Res. Soc.*, **25**, p. 888.
- [40] Woo, S. L.-Y., Simon, B. R., Kuei, S. C., and Akeson, W. H., 1980, "Quasi-Linear Viscoelastic Properties of Normal Articular Cartilage," *ASME J. Biomech. Eng.*, **102**, pp. 85–90.
- [41] Ahmed, A. M., and Burke, D. L., 1983, "In-Vitro Measurement of Static Pressure Distribution in Synovial Joints—Part I: Tibial Surface of the Knee," *ASME J. Biomech. Eng.*, **105**, pp. 216–225.
- [42] Huberti, H. H., and Hayes, W. C., 1984, "Patellofemoral Contact Pressures. The Influence of Q-Angle and Tendofemoral Contact," *J. Bone Jt. Surg., Am. Vol.*, **66A**, pp. 715–724.
- [43] Fung, Y. C., 1981, *Biomechanics: Mechanical Properties of Living Tissues*, Springer-Verlag, New York.
- [44] Mansour, J. M., and Mow, V. C., 1976, "The Permeability of Articular Cartilage Under Compressive Strain and at High Pressures," *J. Bone Jt. Surg., Am. Vol.*, **58A**, pp. 509–516.
- [45] Khalsa, P. S., and Eisenberg, S. R., 1997, "Compressive Behavior of Articular Cartilage Is Not Completely Explained by Proteoglycan Osmotic Pressure," *J. Biomech.*, **30**, pp. 589–594.
- [46] Mak, A. F., 1985, "Uniaxial Tension of Hydrated Viscoelastic Tissues," *ASME Adv. Bioengng.*, N. A. Langrana, ed., pp. 18–19.
- [47] LeRoux, M. A., Ateshian, G. A., Vail, T. P., and Setton, L. A., 2001, "Effects of Collagen Fiber Anisotropy on the Hydraulic Permeability of the Meniscus," *Trans. Orthop. Res. Soc.*, **26**, p. 45.
- [48] Hodge, W. A., Carlson, K. L., Fijan, R. S., Burgess, R. G., Riley, P. O., Harris, W. H., and Mann, R. W., 1989, "Contact Pressures From an Instrumented Hip Endoprosthesis," *J. Bone Jt. Surg., Am. Vol.*, **71A**, pp. 1378–1386.
- [49] Lee, R. C., Frank, E. H., Grodzinsky, A. J., and Roylance, D. K., 1981, "Oscillatory Compressional Behavior of Articular Cartilage and Its Associated Electromechanical Properties," *ASME J. Biomech. Eng.*, **103**, pp. 280–292.
- [50] Kim, Y. J., Bonassar, L. J., and Grodzinsky, A. J., 1995, "The Role of Cartilage Streaming Potential, Fluid Flow and Pressure in the Stimulation of Chondrocyte Biosynthesis During Dynamic Compression," *J. Biomech.*, **28**, pp. 1055–1066.
- [51] Buschmann, M. D., Kim, Y. J., Wong, M., Frank, E., Hunziker, E. B., and Grodzinsky, A. J., 1999, "Stimulation of Aggrecan Synthesis in Cartilage Explants by Cyclic Loading Is Localized to Regions of High Interstitial Fluid Flow," *Arch. Biochem. Biophys.*, **366**, pp. 1–7.